Ionization, Kinematics, and Extent of the Diffuse Ionized Gas Halo of NGC 5775

Richard J. Rand¹

Univ. of New Mexico, Dept. of Physics and Astronomy, 800 Yale Blvd, NE, Albuquerque, NM $87131\,$

ABSTRACT

We present key results from deep spectra of the Diffuse Ionized Gas (DIG) halo of the edge-on galaxy NGC 5775. [N II] λ 6583 has been detected up to $z \approx 13$ kpc above the plane in one of two vertically oriented long slits – making this the spiral galaxy with the greatest spectroscopically detected halo extent in emission. Key diagnostic line ratios have been measured up to $z \approx 8$ kpc, allowing the source of ionization and physical state to be probed. Ionization by a dilute radiation field from massive stars in the disk can explain some of the line ratio behavior, but departures from this picture are clearly indicated, most strongly by the rise of $[OIII]/H\alpha$ with z. Velocities of the gas in both slits approach the systemic velocity of the galaxy at several kpc above the plane. We interpret this trend as a decrease in rotation velocity with z, with essentially no rotation at heights of several kpc. Such a trend was observed in the edge-on galaxy NGC 891, but here much more dramatically. This falloff is presumably due to the gravitational potential changing with z, but will also depend on the hydrodynamic nature of the disk-halo cycling of gas and projection effects. More detailed modeling of the ionization and kinematics of this and other edge-ons will be presented in future papers.

Subject headings: galaxies: individual (NGC 5775) – galaxies: ISM – galaxies: spiral – galaxies: structure – stars: formation

1. Introduction

The Reynolds layer or Warm Ionized Medium of the Milky Way is the repository of about 90% of the free electrons in the ISM. How this medium is ionized, how its large (~ 1 kpc; Haffner, Reynolds, & Tufte 1999) scale height is maintained, and how far it extends vertically are some of the main outstanding issues regarding this diffuse medium. New progress on these issues is being made with the Wisconsin H α Mapper (WHAM; Reynolds et al. 1998). A complementary

¹Visiting Astronomer, National Optical Astronomy Observatories, Tucson, AZ

approach is to examine this medium in external galaxies, where it is generally referred to as Diffuse Ionized Gas (DIG). Narrow-band imaging, spectroscopy, and Fabry-Perot observations have, in recent years, allowed the brightness, spatial distribution, emission line ratios, and kinematics of DIG to be studied in many nearby galaxies (e.g. Golla, Dettmar, & Domgörgen 1994; Greenawalt, Walterbos, & Braun 1997; Hoopes, Walterbos, & Rand 1999; Wang, Heckman, & Lehnert 1997; Rand 1997).

Enhanced ratios of [SII] $\lambda\lambda$ 6716,6731/H α and [NII] $\lambda\lambda$ 6548,6583/H α in the Reynolds layer and external DIG layers relative to HII regions (e.g. Haffner et al. 1999; Golla et al. 1994; Ferguson, Wyse, & Gallagher 1996; Rand 1997) can be explained if the dominant source of ionization is dilute radiation leaked out of star forming regions from massive stars. However, recent high-quality data indicate departures from this simple picture: first, the near constancy with z of [SII]/[NII] in both the Milky Way and external edge-on galaxies (Haffner et al. 1999; Golla et al. 1994; Rand 1998), whereas a rise is expected (e.g. Domgörgen & Mathis 1994; Sembach et al. 2000); second, [SII]/H α and [NII]/H α reach values \gtrsim 1 which are difficult for models to reproduce; and third, [OIII]/H α in the edge-on spiral NGC 891 is found to rise with z (Rand 1998), whereas it is expected to fall as oxygen becomes predominantly singly ionized.

Two explanations for this behavior have been put forth. While viable, both are limited by our knowledge of the energizing sources of halos in general. First, Reynolds, Haffner, & Tufte (1999) and Haffner et al. (1999) have pointed out for the Reynolds layer that the behavior of [S II]/H α , [N II]/H α and [S II]/[N II] could be explained if gas temperature rather than dilution of the ionizing radiation field (and accompanying changes in the ionization state of the metals) were the key parameter that changed with z, since the first two ratios are very temperature sensitive while the third is not. This idea has yet to be applied to an external galaxy. The alternative explanation, which has generally been considered for external galaxies (e.g. Rand 1998; Galarza, Walterbos, & Braun 1999; Martin 1997), is a secondary source of ionization, such as shocks (e.g. Shull & McKee 1979) or turbulent mixing layers (Slavin, Shull, & Begelman 1993) which contribute a fraction of the H α emission which is small but increases with z. The attractive feature of such ionizing sources is that they can yield a high [O III]/H α ratio without necessarily dominating the emission from the other observable lines.

A second issue well addressed in external galaxies is the vertical variation of the DIG kinematics. It has been found in the DIG of NGC 891 that the observed velocities along one vertical slit through the disk become closer to the galaxy systemic velocity with increasing z, suggesting a fall in the rotation speed (Rand 1997). HI data suggest that the effect is widespread in the lower halo (Swaters, Sancisi, & van der Hulst 1997). The rate of falloff will depend on the galactic potential and the hydrodynamic nature of the disk-halo gas cycle (Benjamin 2000).

Finally, of great interest is the detectable extent of DIG layers. DIG in NGC 891 and NGC 5775 has been detected to about z = 5 kpc (Rand 1997; Hoopes et al. 1999), and z = 6 kpc (Collins et al. 2000), respectively, while deep, wide-field imaging of NGC 4631 indicates emission

up to 16 kpc from the plane (Donahue, Aldering, & Stocke 1995).

This paper presents spectra of the edge-on galaxy NGC 5775, which has been previously imaged in the H α line by Collins et al. (2000). It is an interacting galaxy (e.g. Irwin 1994) with a high far infrared luminosity and inferred far infrared surface brightness (Collins et al. 2000) indicating active star formation. Its DIG layer is very bright and extended, as mentioned above, and features some of the most prominent vertical filamentary structure found above a galactic disk. Here we focus on several dramatic new results from these spectra. A full analysis of these data and spectra of three other edge-ons in terms of the two ionization/heating scenarios discussed above will be presented in a future paper (Paper II) by Collins & Rand (in preparation). Another paper (Paper III) will examine the kinematics of the NGC 5775 halo.

2. Observations

The spectra were obtained at the KPNO 4-m telescope on 1999 June 10–13. The slit positions run perpendicular to the plane of the galaxy, as shown in Figure 1, where they are overlaid on the H α image from Collins et al. (2000). The central positions of the slits are given in Table 1. The slit length is 5', the slit width is 2" for the galaxy observations, and the spatial scale is 0.69" per pixel. Slit 1 was chosen to include emission from the most prominent extraplanar DIG filament, while Slit 2 covers a region of weaker emission. The KPC-007 grating was used with the T2KB 2048x2048 CCD, providing a dispersion of 1.42 Å per pixel, a resolution of 3.5 Å, and a useful coverage of 4700 – 6800Å. Many half-hour spectra were taken. Total integration times are given in Table 1.

The basic reduction steps are as described in Rand (1998), and here we only describe processing of the final, stacked, calibrated spectra. Emission from some of the stronger lines extends nearly to the edge of the slit, complicating sky subtraction. In addition, there is a focus variation of unknown origin, causing the lines towards the ends of the slit to be significantly broader than those closer to the center, precluding accurate subtraction of the night sky lines. While the general sky background can still be corrected for, sky lines, when blended with galaxy emission lines, are deconvolved in the line fitting process. This blending was mainly a problem for the H α line, which coincided with a blended pair of sky lines. Towards the ends of the slit, the combined intensity from these sky lines became very constant, indicating that there was no measurable H α and that this intensity value could be used in determining the true H α intensity elsewhere along the slit. A much fainter sky line near [O III] was corrected for in the same way. Strong sky lines also precluded measurements or meaningful upper limits on the [O I] λ 6300 and He I λ 5876 lines for Slit 1, and the [N II] λ 5755 line for both slits.

Line parameters reported here are determined from spectra averaged along the spatial direction, typically by 10 pixels, or 830 pc at an assumed distance of 24.8 Mpc (Irwin 1994). Line properties were determined with Gaussian fits, using a linear fit to the continuum on each

side of the line. For uncertainties on intensities and central wavelengths, the variance of these quantities along each slit for sky lines of a range of intensities were determined, and an estimate of the dependence of these variances on sky line intensity was formed. This relation was then used to determine uncertainties for the emission lines of interest. The detection limit for intensities is about 10^{-18} erg cm⁻² s⁻¹ arcsec⁻².

3. Results

One of the most important results is the tremendous height above the plane to which emission can be detected, providing unique information on the ionization state and kinematics of gas at large distances above the midplane. [NII] $\lambda6583$ is detected to about z=13 kpc and z=7 kpc on both sides of Slits 1 and 2, respectively. H α is detected up to about z=8-9 kpc in Slit 1 and z=6-7 kpc in Slit 2. [O III] $\lambda5007$ is detected to about z=8 kpc on the NE side of Slit 1. The halo of NGC 5775 therefore has the greatest spectroscopically detected extent in emission of any spiral galaxy halo. The vertical emission profiles will be examined in Paper II; we merely point out for the current purposes that, for data averaged over 10 spatial pixels, the H α intensity reaches peak values, in Slits 1 and 2, respectively, of 1.8 and 6.5 $\times10^{-16}$ erg cm⁻² s⁻¹ arcsec⁻², falling by z=5 kpc to 7.5 and 3.8 $\times10^{-18}$ erg cm⁻² s⁻¹ arcsec⁻² (NE and SW values have been averaged together).

Figure 2 shows the vertical runs of the line ratios [S II] $\lambda 6716/\text{H}\alpha$, [N II] $\lambda 6583/\text{H}\alpha$, [S II]/[N II] and [O III] $\lambda 5007/\text{H}\alpha$. Because of the 85° (Irwin 1994) inclination of the galaxy, for points within 10" of the midplane ($z \leq 1200$ pc in the figures), the spatial axis reflects in-plane, highly-inclined disk structure rather than true height above the plane, and line ratio variations are more due to the line of sight crossing HII regions and areas between them. This fact explains why line ratio minima are not always at z=0 kpc.

For the first two ratios, one sees, for the most part, similar behavior to many DIG halos previously observed, although these measurements extend to much larger heights: a general rise with z, with disk values of 0.2–0.3 and halo values of [N II]/H α reaching >1 in places. In general, these ratios rise more slowly with z than in NGC 891. The relatively low and constant values on the NE side of Slit 1 arise from the bright filament, and may simply reflect the well established correlation between these ratios and H α surface brightness (Wang, Heckman, & Lehnert 1998; Rand 1998). In common with the East side of the halo in the spectra of NGC 891 (Rand 1997, 1998), [N II]/H α on the NE side of Slit 1 reaches a maximum at z=6 and subsequently falls, although the maximum is reached at only z=2 kpc in NGC 891. There is a suggestion of similar behavior in both lines on the SW side of Slit 1. [S II]/[N II] is reasonably constant in the halo at a value of about 0.7 in both slits, but shows more variation than in NGC 891, reaching extremes of 0.4 and 1.1.

We examine $[O III]/H\alpha$ rather than $[O III]/H\beta$ since the former can be determined to larger

z. With the exception of the NE side of Slit 2, where it remains relatively constant up to z=4 kpc, this ratio shows a clear increase with z, from values of 0.05–0.4 in the disk to as high as 1.2 in the halo. Unlike the afore-mentioned line ratios, Slit 1 does not show a significant local maximum in this ratio, although the final data point on the SW side suggests that a maximum may have been reached. The behavior is qualitatively similar to NGC 891 (Rand 1998), except that those measurements extended to only z=2 kpc, where a value of $[O\,III]/H\beta=0.8$ was reached. Assuming optically thin gas at 10,000 K, the peak $[O\,III]/H\alpha$ of 1.2 corresponds to $[O\,III]/H\beta=3.7$.

 $[O\,I]/H\alpha$ rises from around 0.02 in the disk to 0.06 at z=2 kpc on the SW side of Slit 2. He I $\lambda 5876$ has been detected in Slit 2, but only for four ten-pixel averages in the disk can meaningful values be measured. The mean of the four $He\,I/H\alpha$ ratios is 0.039 ± 0.003 (the uncertainty is the dispersion of the four values). There is no significant correlation of the ratio with $H\alpha$ intensity.

These data allow halo kinematics to be probed to unprecedented heights. Figure 3 shows velocity centroids of the [N II] $\lambda6583$ and [S II] $\lambda\lambda6716,6731$ lines as a function of slit position for data averaged over ten pixels. The heliocentric systemic velocity, as determined from HI data, is $v_{sys}=1680~{\rm km~s^{-1}}$ (Irwin 1994). Once again, points at $z\lesssim1.2~{\rm kpc}$ represent disk emission. The midplane values in both slits indicate rotation speeds roughly consistent with the rotation curve found by Irwin (1994). The falloff towards v_{sys} for $z\lesssim1.2~{\rm kpc}$ is expected for a differentially rotating disk viewed at a not quite edge-on aspect.

Beyond this point, though, the velocities are of the halo gas. They continue to move closer to v_{sys} with increasing z, coming to within 20 km s⁻¹ of v_{sys} except on the SW side of Slit 1. The simplest explanation of this behavior is that the rotation speed falls with z, as suggested for NGC 891 (Rand 1997), but here becoming roughly consistent with no rotation at the largest heights. The exact translation from observed to rotational velocities is complicated by the unknown distribution of gas along the line-of-sight. This issue will be explored in Paper III. Given the symmetry on either side of the two slits, it is unlikely that the kinematics are dominated by the tidal interaction NGC 5775 is undergoing. For Slit 1, the steeper falloff on the NE side may reflect a receding motion of the prominent filament. In Paper III, we will attempt to constrain the dependence of v_{rot} with z and examine whether the falloff is expected for a reasonable mass model, or whether other hydrodynamical effects (Benjamin 2000) may be important.

4. Discussion

Without carrying out detailed modeling, we can already make conclusions about the possible source(s) of ionization and physical conditions in the DIG that may explain the emission line ratios and their vertical runs. As in NGC 891 and the Reynolds layer, one can already conclude that pure photoionization models will not be able to explain the runs of all the line ratios. Most problematic are the increasing values of $[O\,III]/H\alpha$ with z, in complete contrast to photoionization

models. Also of concern is the relative lack of variation in [S II]/[N II]. Hence, we are led to consider the two possible deviations from the pure photoionization picture discussed in §1. Both may be able to reproduce the trends in these two line ratios, as well as [S II]/H α , [N II]/H α , and [O I]/H α . In Paper II, we will use data on four edge-ons (NGC 891, NGC 5775, UGC 10288, and NGC 4302) to ascertain whether one or the other of these models provides a more adequate description of the data.

Other complications include abundances and the extent to which depletions (e.g. Howk & Savage 1999a) are important, as well as scattering of disk light into the line of sight by extraplanar dust. Absorption due to dust has been shown to be prevalent in several DIG halos (Howk & Savage 1999b). Modeling of NGC 891 (Ferrara et al. 1996) suggests that scattered light is a minor contributor to diffuse halo H α emission (10% at z=600 pc) and declines with z. Nevertheless, scattered light may be significant in some cases.

Apart from the excitation, the kinematics of gaseous halos and the extent to which gas can be expelled from the disk are relevant issues not only to the nature of the disk-halo cycle, but in the interpretation of QSO absorption line systems. For instance, Mg II absorption is probably due to both halos and disks (Charlton & Churchill 1998); consequently possible low-z analogs of absorbers need to be well characterized at faint levels.

The help of the KPNO staff is greatly appreciated. We are also grateful to L. M. Haffner, R. Benjamin, and R. Reynolds for reading a draft of the manuscript.

REFERENCES

Benjamin, R. A., 2000, in Astrophysical Plasmas: Theory, Codes & Models, eds. J. Arthur and J. Franco, Rev. Mex. A. & A., in press.

Charlton, J. C., & Churchill, C. W. 1998, ApJ, 499, 181

Collins, J. A., Rand, R. J., Duric, N., & Walterbos, R. A. M. 2000, ApJ, in press

Domgörgen, H., & Mathis, J. S. 1994, ApJ, 428, 647

Donahue, M., Aldering, G., & Stocke, J. T. 1995, ApJ, 450, L45

Ferguson, A. M. N., Wyse, R. F. G., & Gallagher, J. A. 1996, AJ, 112, 2567

Ferrara, A., Bianchi, S., Dettmar, R.-J., & Giovanardi, C. 1996, ApJ, 467, L69

Galarza, V. C., Walterbos, R. A. M., & Braun, R. 1999, AJ, 118, 2775

Golla, G.; Dettmar, R. -J., & Domgörgen, H. 1994, A&A, 313, 439

Greenawalt, B., Walterbos, R. A. M., & Braun, R. 1997, ApJ, 483, 666

Haffner, L. M., Reynolds, R. J., & Tufte, S. L. 1999, ApJ, 523, 223

Hoopes, C. G., Walterbos, R. A. M., & Rand, R. J. 1999, ApJ, 522, 669

Howk, J. C., & Savage, B. D. 1999a, ApJ, 517, 746

Howk, J. C., & Savage, B. D. 1999b, AJ, 117, 2077

Irwin, J. A. 1994, ApJ, 429, 618

Martin, C. L. 1997, ApJ, 491, 561

Rand, R. J. 1997, ApJ, 474, 129

Rand, R. J. 1998, ApJ, 501, 137

Reynolds, R. J., Tufte, S. L., Haffner, L. M., Jaehnig, K., & Percival, J. W. 1998, PASA, 15, 14

Reynolds, R. J., Haffner, L. M., & Tufte, S. L. 1999, ApJ, 525, L21

Sembach, K. R., Howk, J. C., Ryans, R. S., & Keenan, F. P. 2000, ApJ, 528, 310

Shull, J. M., & McKee, C. F. 1979, ApJ, 227, 131

Slavin, J. D. Shull, J. M. & Begelman, M. C. 1993, ApJ, 407, 83

Swaters, R. A., Sancisi, R., & van der Hulst, J. M. 1997, ApJ, 491, 140

Wang, J., Heckman, T. M., & Lehnert, M. D. 1997, ApJ, 491, 114

Wang, J., Heckman, T. M., & Lehnert, M. D. 1998, ApJ, 509, 93

This preprint was prepared with the AAS LATEX macros v4.0.

Table 1: Summary of the Observations

| Slit | Offset along | Hours of | $ m Noise^{b}$ |
|------|-------------------------|-------------|---|
| | Major axis ^a | Integration | $(10^{-19} \text{ erg cm}^{-2} \text{ s}^{-1} \text{ Å}^{-1} \text{ pix}^{-1})$ |
| 1 | 32" NW | 6 | 3.1 |
| 0 | 20" SE | - | 3.3 |

a Offsets are from the HI kinematic center determined by Irwin (1994) at R.A. $14^{\rm h}$ $53^{\rm m}57.6^{\rm s}$, Dec. 3° 32' 40" (2000.0). b Angular pixel size is 1.38 arcsec². An intensity of 2×10^{-18} erg cm⁻² s⁻¹ arcsec⁻² corresponds to an Emission Measure of 1 pc cm⁻⁶

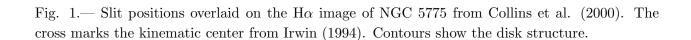


Fig. 2.— Dependence of line ratios on slit position for Slit 1 (filled circles) and Slit 2 (open circles). Line ratios plotted are (a) [S II] $\lambda 6716/\text{H}\alpha$, (b) [N II] $\lambda 6583/\text{H}\alpha$, (c) [S II]/[N II] and (d) [O III] $\lambda 5007/\text{H}\alpha$. Although the position axis is labeled z, note that points at $z \lesssim 1200$ pc reflect in-plane structure more than vertical structure.

Fig. 3.— The intensity-weighted mean heliocentric velocities of the [N II] $\lambda 6583$ and [S II] $\lambda \lambda 6716,6731$ lines as a function of position for (a) Slit 1 and (b) Slit 2. The dashed line indicates the systemic velocity.

